Overcoming the Diffraction Limit with a Planar Left-Handed Transmission-Line Lens

Anthony Grbic and George V. Eleftheriades

The Edward S. Rogers Sr. Department of Electrical and Computer Engineering, University of Toronto,
10 King's College Road, Toronto, Ontario, Canada M5S 3G4
(Received 28 May 2003; published 18 March 2004)

We report experimental results at 1.057 GHz that demonstrate the ability of a planar left-handed lens, with a relative refractive index of −1, to form images that overcome the diffraction limit. The left-handed lens is a planar slab consisting of a grid of printed metallic strips over a ground plane, loaded with series capacitors (C) and shunt inductors (L). The measured half-power beamwidth of the point-source image formed by the left-handed lens is 0.21 effective wavelengths, which is significantly narrower than that of the diffraction-limited image corresponding to 0.36 wavelengths.

Classical electrodynamics imposes a resolution limit when imaging using conventional lenses. This fundamental limit, called the diffraction limit, in its ultimate form is attributed to the finite wavelength of electromagnetic waves. The electromagnetic field emanating from a line source lying along the y axis consists of a continuum of plane waves $e^{ik_x x} e^{ik_z z}$. Each plane wave has a characteristic amplitude and propagates at an angle with the optical z axis given by the direction cosine (k_z/k), where k is the propagation constant in the medium. The plane waves with real-valued direction cosines $(k_x \leq k)$ propagate without attenuation, while the evanescent plane waves with imaginary direction cosines $(k_x > k)$ attenuate exponentially along the optical z axis. A conventional lens focuses only the propagating waves, resulting in an imperfect image of the object. The finer spatial details (smaller than a wavelength) of the object, carried by the evanescent waves, are lost due to the strong attenuation these waves experience ($e^{-z\sqrt{k_x^2 - k^2}}$) when traveling from the object to the image. Therefore, only plane waves with transverse wave numbers in the range $0 \leq |k_x| \leq k_{max} = k$ contribute to the image. This loss of evanescent spectrum, which occurs even for an infinitely large lens, constitutes the origin of the diffraction limit in its ultimate form. The minimum resolvable feature Δx is given by the Fourier transform relationship $k_{max}\Delta x \sim 2\pi$. Therefore, $\Delta x \sim 2\pi/k = \lambda$ and the diffraction limit manifests itself as an image smeared over an area approximately one wavelength in diameter.

In 2000, Pendry predicted that lenses made out of flat slabs of left-handed materials (materials with negative permittivity and permeability) could overcome the diffraction limit [1]. These left-handed materials were first envisioned by Veselago in the 1960s [2] and shown to exhibit a negative index of refraction. Pendry suggested that left-handed slabs allow "perfect imaging" if they are completely lossless, impedance matched, and their refractive index is −1 relative to the surrounding medium. The left-handed lens achieves perfect imaging by focusing propagating waves as well as supporting growing evanescent waves which restore, at the image plane, the decaying evanescent waves emanating from the source. In 2001, a group at University of California–San Diego led by Smith and Schultz experimentally demonstrated negative refraction at microwave frequencies using a left-handed medium made of an array of unit cells consisting of split-ring resonators and wires (SRR/wire) [3]. Recently, improved experimental results verifying negative refraction have been reported using the same SRR/wire medium [4]. Nevertheless, experimental focusing using SRR/wire left-handed lenses suffered high transmission losses and focusing that surpasses the diffraction limit has remained elusive [5]. In fact, the ability to overcome the diffraction limit was questioned theoretically [6] and in simulation [7]. Overcoming the diffraction limit involves restoring some of the source's evanescent spectrum at the image plane. In other words, the field at the image plane includes plane waves with $0 \leq |k_x| \leq k_{max}$, where $k_{max} > k$. The minimum resolvable feature $\Delta x \sim 2\pi/k_{max}$ then becomes smaller than a wavelength. Hence, a resolution enhancement $R = k_{max}/k$ can be defined for a practical left-handed lens [8].

A different approach for synthesizing planar isotropic (perpendicular electric field polarization) left-handed media has been described by Eleftheriades *et al.* in 2002. The approach is based on two-dimensional transmission-line (TL) grids loaded with series capacitors (C) and shunt inductors (L) as shown in Fig. 1(a) [9]. Using this L-C loaded TL approach, focusing from a homogeneous dielectric to a left-handed TL medium was demonstrated experimentally at microwave frequencies [9,10]. In addition, radiating versions of these media have been used to experimentally demonstrate backward-wave radiation in free space [11]. It is important to note that the experimental lenses reported in [9,10] utilized a single interface between a left-handed medium and a homogeneous dielectric. This arrangement did not permit the proper growth of evanescent waves necessary to clearly observe imaging beyond the diffraction limit. Subsequently, planar slabs (having two interfaces) of L-C loaded TL

(a) Loaded Grid

(Left-Handed

Medium)

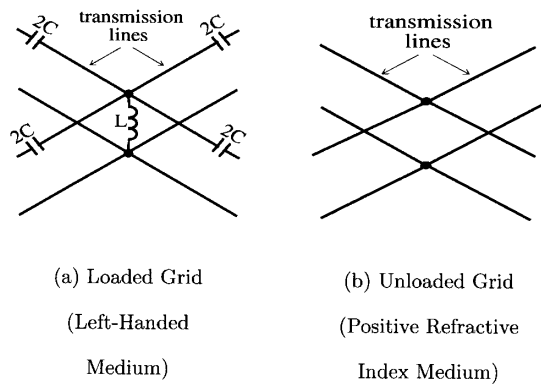(b) Unloaded Grid

(Positive Refractive

Index Medium)

FIG. 1.   Transmission line unit cells.

left-handed media were shown, in simulation, to support growing evanescent waves, the key to overcoming the diffraction limit [12]. In this work, a planar left-handed slab as described in [12] has been constructed and tested to demonstrate imaging beyond the diffraction limit at microwave frequencies.

The experimental structure is illustrated in Fig. 2. It is fabricated on a grounded microwave substrate (Rogers RO3003) of thickness 60 mil (1.52 mm) and dielectric constant $\epsilon_r = 3.00$. The left-handed slab consists of a 5×19 grid of printed copper strips (microstrip transmission lines) loaded with series chip capacitors C and shunt (to the ground) chip inductors L. A TL schematic of the loaded grid's unit cell is shown in Fig. 1(a), where the transmission lines represent the printed strips of the grid. In the design, $C = 2.7$ pF (ATC 500S) and $L = 18$ nH (Toko LL1608FH) inductors are used. The printed strips have a metal thickness of 17 μm and are 750 μm wide. Furthermore, each unit cell has dimensions $d \times d = 8.40 \times 8.40$ mm. Essentially, the loaded periodic grid acts as a left-handed isotropic and homogeneous medium
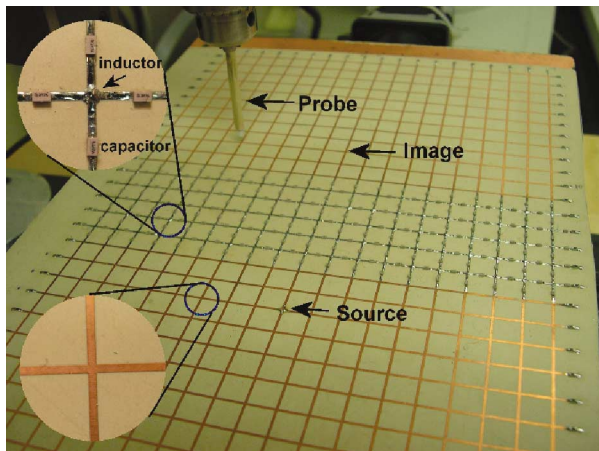

FIG. 2 (color).   The left-handed planar transmission-line lens. The unit cell of the left-handed (loaded) grid is shown in the top inset, while the unit cell of the positive-refractive-index (unloaded) grid is shown in the bottom inset.

exhibiting a negative index of refraction [9,10,12]. The loaded grid is sandwiched between two commensurate unloaded printed grids (each 12×19 cells) that act as effective homogeneous media with a positive index of refraction. A TL schematic of the unloaded grid's unit cell is shown in Fig. 1(b). The unit cell dimensions and printed strips of the two unloaded grids are identical to those used in the loaded grid.

The left-handed loaded grid was designed so that it is impedance matched and exhibits a refractive index of -1 relative to the unloaded grids at the design frequency of 1.00 GHz [12]. To achieve a relative refractive index of -1, the effective wave numbers of the unloaded grid and loaded grid were designed to be equal in magnitude but opposite in sign at 1.00 GHz [12]. The effective wave numbers were designed to be $k_1 = k$ in the unloaded grid and $k_2 = -k$ in the loaded grid shown in Fig. 2, where $k = 40.31$ rad/m. These wave numbers correspond to an effective wavelength ($\lambda = 2\pi/k$) of 15.59 cm and an index of refraction of 1.925 in the unloaded grid and -1.925 in the loaded grid at 1 GHz. The Bloch impedance Z_B (in the direction of power flow) for propagating waves was designed to be 90.000 Ω for both the loaded and unloaded grids.

In the experiment, the first unloaded grid is excited with a vertical monopole fed by a coaxial cable through the ground plane. The monopole attaches the center conductor of the coaxial cable to a point on the unloaded grid, while the outer conductor of the coaxial cable attaches to the ground plane. This vertical monopole lies along the central row (row 0), located 2.5 cells (0.135λ) away from the first interface of the left-handed slab (see Fig. 2). The source and image are symmetrically positioned with respect to the left-handed slab since the distance from the source to the first interface (2.5 cells) is half the left-handed slab thickness (5 cells) [2]. In essence, the setup shown in Fig. 2 is a practical implementation for imaging an elemental source from one homogeneous dielectric to another using a left-handed slab. The unloaded grid over the ground plane behaves like a dielectrically loaded parallel-plate waveguide, but in addition permits the simple measurement of the guided fields through proximity coupling.

The vertical electric field is detected 0.8 mm above the entire surface of the structure, using a short vertical probe connected to a Hewlett-Packard vector network analyzer model 8753D. Port 1 of the network analyzer is connected to the coaxial cable that feeds the exciting monopole. Port 2 is connected by a separate coaxial cable to the detecting probe that is scanned above the surface of the structure using a computer-controlled stepper motor [10]. The measured transmission coefficient is proportional to the voltage of the grid nodes with respect to the ground plane. The best focusing results were observed at 1.057 GHz, a frequency slightly higher than the design frequency of 1.00 GHz. This is primarily due to the

variation in chip inductors and capacitors from their nominal values, as well as fabrication tolerances in printing the grid lines. The measured vertical electric field above each unit cell for the entire structure is shown in Fig. 3, at a frequency of 1.057 GHz. The source is located at (column, row) = (0, 0) and the image at (10, 0), whereas the first interface is between columns 2 and 3 and the second interface is between columns 7 and 8. As shown, the enhancement of evanescent waves is quite evident at the second interface of the left-handed slab near the central row (row 0). Figure 4 explicitly shows the measured electric field along row 0 to emphasize the growing evanescent fields within the left-handed lens. The measured vertical electric field along the image column (column 10) is shown in Fig. 5. Plotted in the same figure is the measured electric at the source column (column 0), as well as the theoretical diffraction-limited pattern in a continuous medium and the diffraction-limited pattern in a periodic TL grid medium with the same effective material parameters. All patterns in Fig. 5 are normalized to unity for comparison purposes. Nevertheless, the measured source and image peaks lie within 7% of each other. Because of the close proximity (0.54λ) of the source and its image, evanescent waves that reach the image are accounted for in the theoretical diffraction-limited patterns. The diffraction-limited patterns assume that the propagating plane wave components are focused whereas the evanescent components are assumed to exponentially decay from the source to the image, corresponding to a refractive index of $n = +1.925$. The diffraction-limited voltage (V) at the image plane (column 10) in a continuous medium is given by Eq. (1):

$$V(x) = C \int_{-\infty}^{-\infty} \frac{e^{ik_{z1}t}e^{ik_{z2}t}e^{ik_x x}}{k_{z1}} dk_x,$$

$$k_{z1} = -k_{z2} = \sqrt{k^2 - k_x^2} \quad \text{for } k_x < k, \qquad (1)$$

$$k_{z1} = k_{z2} = i\sqrt{k_x^2 - k^2} \quad \text{for } k_x > k,$$

where C is a constant that normalizes $V(0) = 1$, $t = 5d = 42.0$ mm is the thickness of the lens, and $k = 40.31$ rad/m. The half-power beamwidth of the diffraction-limited pattern shown in Fig. 5 is 0.36 wavelengths. The second diffraction-limited pattern accounts for the periodicity ($d = 8.4$ mm) of the TL grid media with Z_B and k as previously defined. Both of these diffraction-limited patterns are practically identical to the far-field diffraction-limited pattern that completely neglects evanescent waves. This suggests that the distance between source and image (0.54λ) is sufficiently large such that evanescent waves passing through a conventional lens would not reach the image plane. Therefore, any enhancement in image resolution can be attributed to the left-handed lens's ability to restore evanescent waves at the image plane.
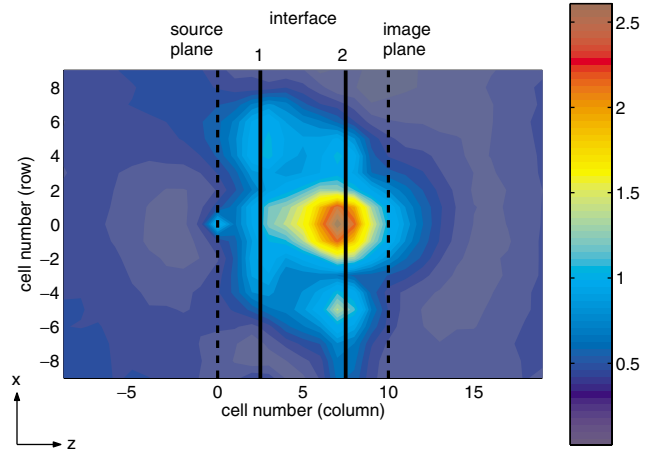

FIG. 3 (color). The measured vertical electric field detected 0.8 mm above the surface of the entire structure at 1.057 GHz. The plot has been normalized with respect to the source amplitude (linear scale).

The measured image is evidently narrower than the diffraction-limited patterns. The measured half-power beamwidth is 0.21 effective wavelengths compared to 0.36 wavelengths for the diffraction-limited patterns. This narrowing of the beamwidth beyond the diffraction limit is due to the growing evanescent waves evident in Figs. 3 and 4. Nevertheless, the image is still imperfect since the source beamwidth is narrower than that of the image. This is not surprising considering that several recent papers have shown that mismatches at the lens interfaces due to slight material losses or deviations in material parameters significantly degrade the resolution enhancement R [8,10,13].

The analytical treatment of imaging using loaded TL grids presented in [14] was utilized to investigate the resolution enhancement R of the experimental lens. This analysis predicts the nodal voltages in left-handed planar TL lenses such as the one shown in Fig. 2. In [14] it is shown that R is limited by the periodicity of a lossless
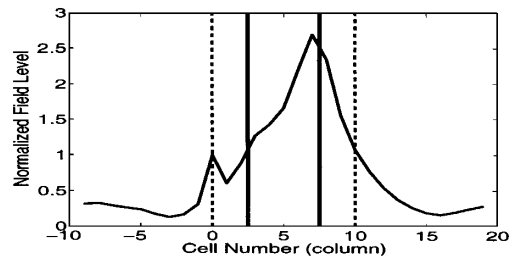

FIG. 4. The measured vertical electric field above row 0 at 1.057 GHz. The vertical dashed lines identify the source (column 0) and image (column 10) planes while the vertical solid lines identify the interfaces of the left-handed planar slab. The growth of the evanescent waves in the left-handed lens is clear.
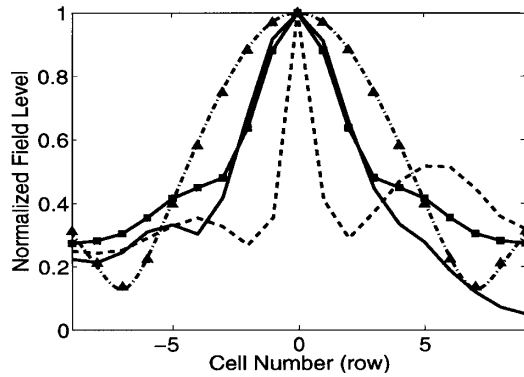
FIG. 5. The measured vertical electric field at the source (dashed curve) and the image (solid curve) planes along with the theoretical diffraction-limited patterns in a continuous medium (dash-dotted curve) and a periodic TL grid medium (triangles) as well as the computed loss-limited image (squares). The measured source and image peaks lie within 7% of each other but have been normalized to 1.

planar TL lens in the following manner: $R = \pi/kd$. For the experimental lens, the maximum resolution enhancement due to the periodicity is $R = \pi/(0.3386) = 9.3$. Therefore, if the experimental lens were lossless, the image would include transverse wave numbers in the range $0 \leq |k_x| \leq 9.3k$. Losses were then included into the analytical treatment in order to predict how they degrade the experimental image beamwidth and resolution. The loss in the unloaded grid was estimated by finding the losses on the interconnecting microstrip lines using Agilent's transmission-line calculator Linecalc. The estimated refractive index for the unloaded grid is $n = 1.9246 + 0.0044i$. The unloaded grid parameters are estimated to be $k = 40.3088 + 0.0918i$ rad/m and $Z_B = 90.0001 + 0.0030i$ Ω. The loss in the loaded grid was estimated by considering the microstrip lines and the quality factors of the inductors ($Q = 44$ at 1 GHz) and capacitors ($Q = 150$ at 1 GHz) used in the experiment. The estimated refractive index for the loaded grid is $n = -1.9238 + 0.0599i$. The low inductor Q is the primary cause of the imaginary part of the refractive index. The loaded grid parameters are estimated to be $k = -40.2917 + 1.2538i$ rad/m and $Z_B = 89.9882 - 1.4140i$ Ω.

Incorporating these losses into the analytical treatment [14] resulted in a computed (loss-limited) image that has the same beamwidth as the experimental image (see Fig. 5). Fourier transforming either of these two images reveals that only transverse wave numbers in the range $0 \leq |k_x| \leq 3k$ form the image. Therefore, the resolution enhancement of the experimental lens is $R = 3$.

These experimental results support the physics behind Pendry's "perfect lens." We have demonstrated that despite the sensitivity of left-handed lenses to manufacturing tolerances and material losses, it is still possible to achieve subdiffraction imaging.

[1] J. B. Pendry, Phys. Rev. Lett. **85**, 3966 (2000).
[2] V. G. Veselago, Sov. Phys. Usp. **10**, 509 (1968).
[3] R. A. Shelby, D. R. Smith, and S. Schultz, Science **292**, 77 (2001).
[4] C. G. Parazzoli, R. B. Greegor, K. Li, B. E. C. Koltenbah, and M. Tanielian, Phys. Rev. Lett. **90**, 107401 (2003).
[5] A. A. Houck, J. B. Brock, and I. L. Chuang, Phys. Rev. Lett. **90**, 137401 (2003).
[6] N. Garcia and M. Nieto-Vesperinas, Phys. Rev. Lett. **88**, 207403 (2002).
[7] P. F. Loschialpo, D. L. Smith, D. W. Forester, F. J. Rachford, and J. Schelleng, Phys. Rev. E **67**, 025602 (2003).
[8] D. R. Smith, D. Schurig, R. Rosenbluth, S. Schultz, S. A. Ramakrishna, and J. B. Pendry, Appl. Phys. Lett. **82**, 1506 (2003).
[9] G. V. Eleftheriades, A. K. Iyer, and P. C. Kremer, IEEE Trans. Microwave Theory Tech. **50**, 2702 (2002).
[10] A. K. Iyer, P. C. Kremer, and G. V. Eleftheriades, Opt. Express **11**, 696 (2003).
[11] A. Grbic and G. V. Eleftheriades, J. Appl. Phys. **92**, 5930 (2002).
[12] A. Grbic and G. V. Eleftheriades, Appl. Phys. Lett. **82**, 1815 (2003).
[13] N. Fang and X. Zhang, Appl. Phys. Lett. **82**, 161 (2003).
[14] A. Grbic and G. V. Eleftheriades, IEEE Trans. Microwave Theory Tech. **51**, 2297 (2003).